Solar Energy Materials and Solar Cells 200 (2019) 110000

Contents lists available at ScienceDirect

Solar Energy Materials and Solar Cells

journal homepage: www.elsevier.com/locate/solmat

Thermally stable electrochromic devices using Fe(II)-based metallo-supramolecular polymer

Sanjoy Mondal, Takefumi Yoshida, Utpal Rana, Manas Kumar Bera, Masayoshi Higuchi*

Electronic Functional Macromolecules Group, National Institute for Materials Science (NIMS), 1-1 Namiki, Tsukuba, 305-0044, Japan

ARTICLE INFO

Keywords:
Electrochromic device
Polymeric gel electrolyte
Counter material
Film thickness
Device durability
Thermal stability

ABSTRACT

A solid-state electrochromic (EC) device with high thermal durability was successfully fabricated by the combination of Fe(II)-based metallo-supramolecular polymer (polyFe) as a cathodically coloring EC layer, a poly (methyl methacrylate)-based solid-state electrolyte layer, and Prussian blue (PB) as an anodically coloring EC layer between two indium tin oxide (ITO)-coated glass conducting substrates. Spray coating technique was used to make polyFe film on ITO-glass. Counter materials were investigated to improve the long-term durability and performance of solid state devices. The polyFe layer thickness was optimized at 240 ± 50 nm, resulting in better electrochromic performance of the fabricated device with transmittance change of ~54% and 95% cyclic stability after 1000 cycles with a short response time by applying voltages of +2.7 V and −1.3 V reversibly. Importantly, the thermal stability of the fabricated solid device was also explored, and we achieved maximum temperature stability at 100 °C with 50% retention of device properties in this study.

1. Introduction

Recently, the development of highly durable, thermally stable, and efficient electrochromic devices has emerged as an important research topic worldwide, owing to the incredible requirements of high-demand applications [1–5]. Due to the controllable optical properties of EC devices, they can be used in different applications such as anti-glare rearview windows [6], information displays [7], and windows designed for sunlight attenuation [8]. Apart from these applications, EC devices can be used as energy saving smart windows for buildings, vehicles, etc. [9,10]. Various kinds of materials are used as the electrochromic materials for EC device fabrication, such as metal oxides [11,12], small organic molecules [13,14], viologens [15,16], and conductive polymers [17,18], including metallo-supramolecular polymers (MSPs) [19,20]. Several kinds of electrochromic materials have already been developed to yield good color contrast, short switching time, and different color variations [11–20]. However, some drawbacks or imperfections must still be overcome for commercialization; improvements in durability and thermal stability are necessary.

An electrochromic device showing a color change in the chromic layer generally consists of an electrolyte in between two conducting substrates. Importantly, the choice of electrolyte is one of the important factors for fabricating highly durable, weather resistant electrochromic devices. Usually, conventional electrochromic devices are operated by a liquid electrolyte or low-viscosity gel electrolyte; however, safety issues have limited their application. Interestingly, replacing liquid electrolyte with a highly viscous gel or solid electrolyte is essential for lightweight, safe, thin, handy electrochromic devices [21–24]. An electrochromic device based on a solid polymeric electrolyte effectively resolves the electrolyte leakage and short-circuit problems, increases the mechanical strength and electrochemical stability of the device, and brings many other benefits. Different types of polymers have been investigated for making solid polymeric electrolytes for electrochromic devices, including poly(vinylidene fluoride) (PVdF) and its derivatives, poly (ethylene oxide) (PEO), and poly(methyl methacrylate) (PMMA) [24,25]. Recently, room-temperature ionic liquids have been proposed as promising nonvolatile, solvent-free, highly conducting electrolytes, but high costs have restricted their application [26,27]. In addition to the electrolyte, the counter electrode is also an important part of an electrochromic device that plays a significant role in solid-state device performance with respect to device fast step switching, durability, steady current flow for long durations, and so on [28–30]. A counter electrode or counter electrode materials should serve as a charge storage layer during the reversible redox change which occurs when a bias voltage is applied to the device. In an electrochromic device, a redox reaction occurs in the working electrode, and exactly opposing redox reactions should occur simultaneously at the counter electrode side. These simultaneous but opposite redox reactions in the working and

* Corresponding author.
E-mail address: HIGUCHI.Masayoshi@nims.go.jp (M. Higuchi).

https://doi.org/10.1016/j.solmat.2019.110000
Received 18 January 2019; Received in revised form 30 April 2019; Accepted 9 June 2019

counter electrode lead to easy and steady current flow through the device, which improves long-term cyclic performance in low potential windows. There are several kinds of materials that can be used as the counter electrode, such as nickel hexacyanoferrate (NiHCF) [31,32], zinc hexacyanoferrate (ZnHCF) [33], copper hexacyanoferrate (CuHCF) [34], Prussian blue (PB) [35,36], conducting polymers [37,38], etc. However, the selection of the proper counter electrode material for a polyFe electrochromic layer based solid-device is an important issue.

Here, we report the fabrication of a solid-state electrochromic device based on a previously synthesized Fe(II)-metal centered metallo-supramolecular polymer (polyFe) [19,20] as an electrochromic layer on the working electrode side, a novel solid polymeric gel composed of $LiClO_4$, PMMA, and PC as the electrolyte layer, and anodically coloring PB as an ion storage layer on the counter electrode side. A facile, low-cost, nontoxic technique has been investigated to fabricate this solid-state electrochromic device. The fabricated electrochromic device showed excellent electrochromic performance within an operating voltage range of +2.7 V/-1.3 V. The effect of the counter electrode material on long-term durability was investigated. The thickness of polyFe has been optimized to improve the electrochromic performance of the device in terms of cyclic stability, transmittance change, and response time. We have achieved a maximum transmittance change (ΔT) of ~54% for a polyFe film thickness of 240 ± 50 nm with 95% cyclic stability after 1000 cycles at room temperature. Furthermore, we have measured the high-temperature cyclic stability of the fabricated device in the range of 50–100 °C. The device retained 50% of its electrochromic properties after cycling under conditions of 100 °C and 40% relative humidity (RH).

2. Experimental section

2.1. Materials and instruments

Iron(II) acetate [$Fe(OAc)_2$ > 99.99%], indium tin oxide (ITO)-coated glass substrates (resistivity 8–12 Ω/sq.), anhydrous lithium perchlorate ($LiClO_4$), and PB ($Fe_4[FeCN_6]_3$) were purchased from Sigma Aldrich. 1,4-Di[[2,2':6',2"-terpyridin]-4'-yl]benzene and poly-(methyl methacrylate) [PMMA, MW 350 kg/mol] were purchased from TCI Chemical. Propylene carbonate (PC), anhydrous acetic acid, spectroscopic grade methanol (MeOH), and acetonitrile (ACN) were supplied by Wako Chemicals.

All electrochemical studies were carried out using an ALS/CHI electrochemical workstation (CH Instruments, Inc.) using a two-electrode system. An integrated Ocean Optics modular spectrometer was connected with electrochemical analyzer to monitor transmittance change in the EC devices upon application of potential. An Apeiros API Corporation automated spray coater was used for polyFe film preparation. A Veeco Instruments Inc. (Model Dektak 6 M) surface profiler was used for polyFe thickness measurement. An ESPEC Corp. benchtop-type chamber (SH-242) was used as a temperature and humidity control chamber. The surface topology of spray coated polyFe film was studied using atomic force microscopy (AFM) in dynamic mode using a Si-DF40 cantilever (Nano Navi II of Seiko Instruments Inc. SII). Thermogravimetric analysis (TGA) was performed by using an SII TG/DTA 6200 instrument in a N_2 environment with a 10 °C/min heating rate. A Solartron 1260 impedance gain/phase analyzer coupled with a Solartron 1296 dielectric interface was used for AC impedance measurements at ambient conditions.

2.2. Preparation of polyFe

PolyFe was synthesized according to our previously reported procedure [19,20]. In this procedure, equimolar amounts of 1,4-di[[2,2':6',2"-terpyridin]-4'-yl]benzene (200 mg, 0.37 mmol) and Fe$(OAc)_2$ (64 mg, 0.37 mmol) were refluxed in a N_2-saturated atmosphere in an acetic acid medium for 24 h. After cooling the reaction mixture down to room temperature, the small amount of insoluble residue was removed by filtration. The deep blue filtrate solution was transferred to a petri-dish and the acetic acid solvent was evaporated slowly at room temperature under atmospheric conditions. Finally, the product was further dried under vacuum to yield a deep-blue colored solid polyFe with ~90% yield.

2.3. PolyFe film preparation on ITO-glass

Firstly, polyFe was dissolved in MeOH to form a 3.5 mg/mL solution and stirred for 2 h at room temperature. Prior to the preparation of polymer films, the polymer solution was filtered by a syringe filter (PVDF, 0.45 μm) to completely remove any small insoluble residue. Before the preparation of polymer films, the ITO-glass substrates were cleaned by ultrasonication in acetone for 10 min and then exposed to ultraviolet-ozone for 20 min. Before spray coating, ITO-glass substrates were placed on a hotplate (temperature 60–70 °C). Smooth and uniform blue colored polyFe films were prepared using an automated spray coater on 2.5 × 2.5 cm^2 ITO-glass substrates. By changing the spray coating speed to 500, 400, 300, and 200 rpm for a single coating repetition and fixed solution concentration (3.5 mg/mL), we made films with four different thicknesses, viz. Film-1, Film-2, Film-3, and Film-4 (Table S1, Supplementary data).

2.4. PB film preparation on ITO-glass

Similarly, PB films were prepared on ITO-glass substrates after cleaning in acetone and UV-Ozone. Very thin PB layers were prepared on 2.5 × 2.5 cm^2 ITO-glass substrates by spin coating with a spin speed of 1500 rpm for 30 s from a water solution of PB (10 mg/mL).

2.5. Preparation of gel electrolyte and device fabrication

A viscous gel electrolyte was prepared by mixing $LiClO_4$ in PC with vigorous stirring for 30 min. After the $LiClO_4$ completely dissolved in PC, solid PMMA was added to the solution with constant stirring. We maintained the component weight ratio in the viscous solution as $LiClO_4$/PC/PMMA = 8/46/46. The viscous solution was stirred under reduced pressure at room temperature for 1 h to removed dissolved air-bubbles from the solution. Next, the viscous solution was poured onto polyFe coated ITO-glass substrates (working electrode). After that, the gel was sandwiched between (i) two bare ITO-glass layers to form the Type-I device and (ii) two PB-coated ITO-glass layers to form the Type-II device. The resulting two types of devices were placed in a temperature/humidity control chamber at 100 °C and 40% relative humidity (RH). Once the chamber temperature reached 100 °C, the chamber temperature was cooled down to 25 °C at 40% RH. Finally, the devices were cleaned and sealed with silicon glue to protect them from atmospheric conditions. Different voltages were applied to the positive and negative electrodes to observe any color change in the device.

3. Results and discussion

The synthesized polyFe was characterized by UV–Vis spectroscopy, atomic force microscopy (AFM), and thermogravimetric analysis (TGA). The chemical structural changes in polyFe during oxidation and reduction are shown in Fig. 1a. The methanol solution of polyFe shows a strong absorption peak at ~580 nm (Fig. 1b) in its UV–Vis spectrum, attributed to the metal-to-ligand-charge-transfer (MLCT) transition of the central Fe^{2+}-metal ion to terpyridine ligands to form a quasi-octahedral coordination geometry [19,20,39,40]. The surface morphology and roughness of the spray coated polyFe film were examined by AFM (Fig. 1c and d). AFM analysis clearly showed a rough cloudy like surface in a 2.5 × 2.5 μm^2 area range. The thermal stability was also measured by a TGA study and it remained quite stable up to 350 °C as shown in Fig. S1 (Supplementary data). In the TGA study, a small

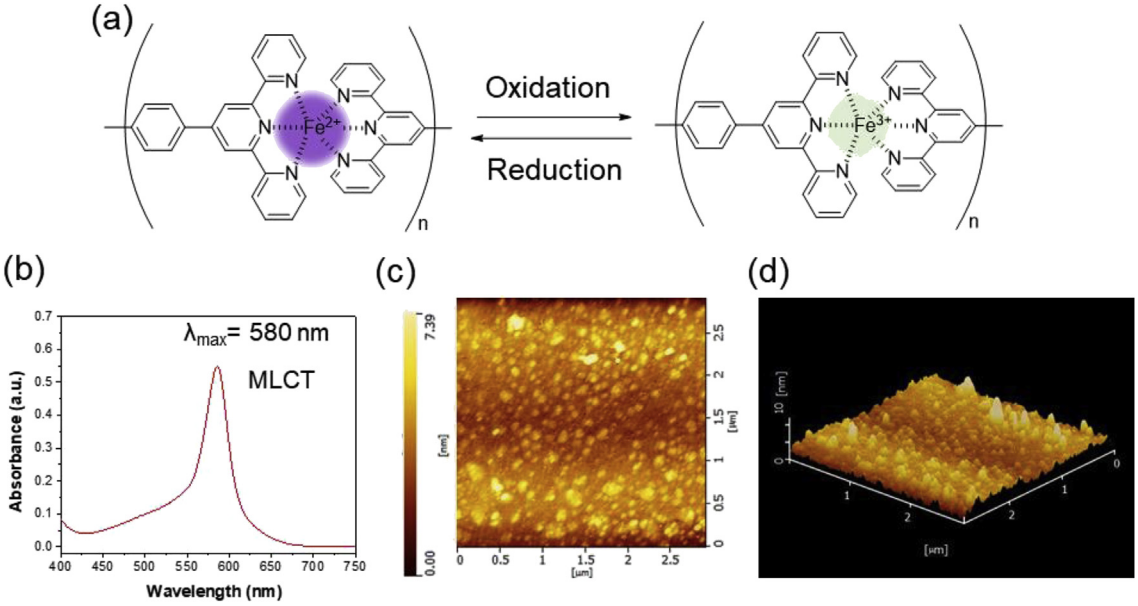

Fig. 1. (a) Chemical structure of polyFe in oxidized and reduced forms. (b) UV–Vis spectra of polyFe in methanol solution. (c, d) AFM image and the corresponding height profile view of the spray-coated film.

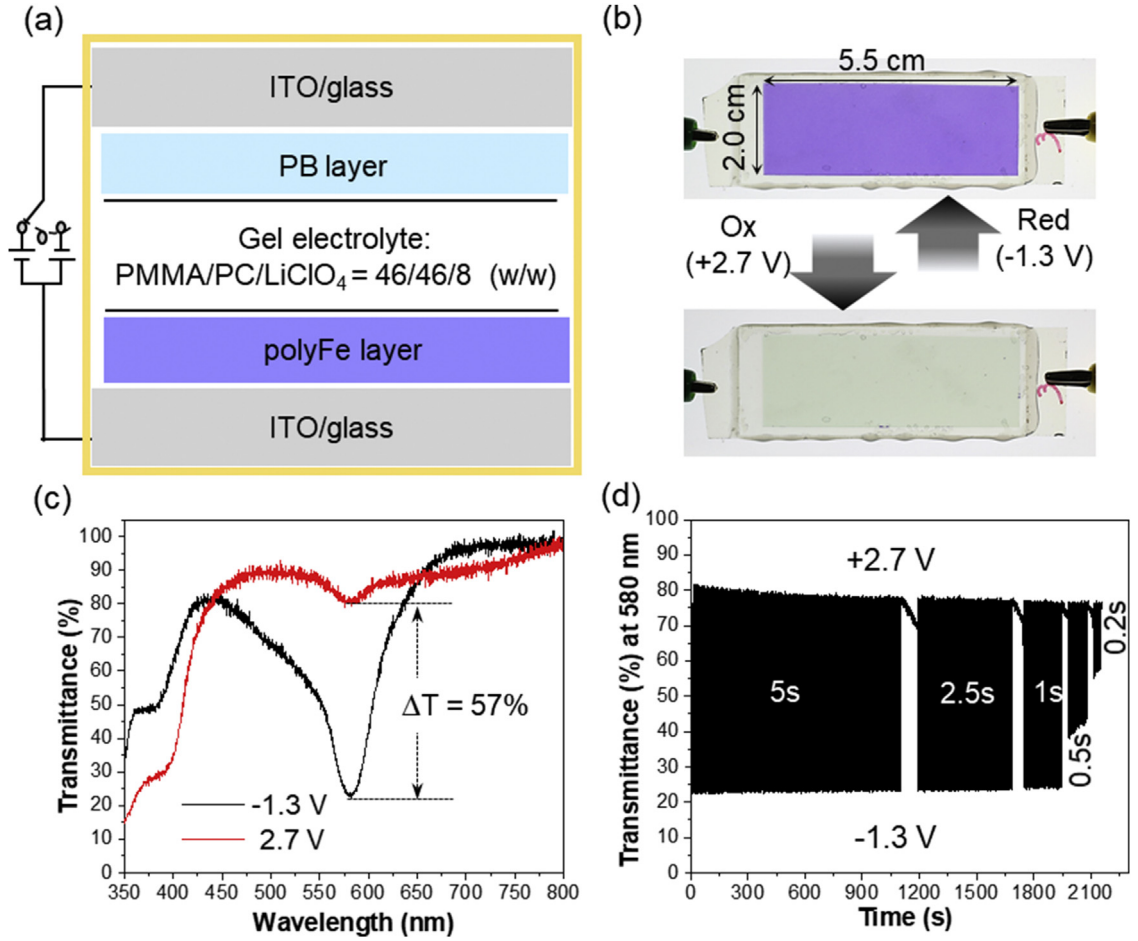

Fig. 2. (a) Design of the fabricated solid-state electrochromic device. (b) Reversible color change on device (dimension 2.0 × 5.5 cm^2). (c) Spectral change of transmittance (T%) for the solid-state device by applying a voltage of +2.7 V and −1.3 V. (d) Change of transmittance (ΔT %) for solid-sate device by applying the same voltage with different intervals (5 s, 2.5 s, 1 s, 0.5 s, and 0.2 s respectively).

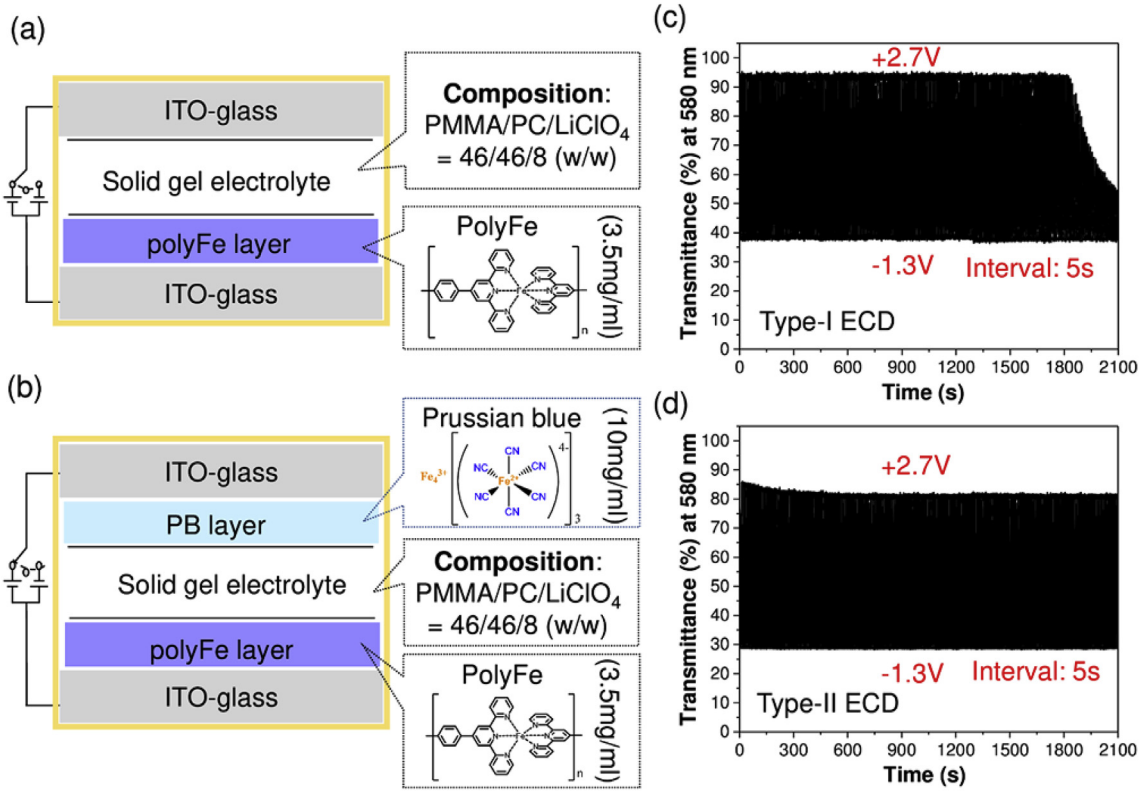

Fig. 3. Design of the fabricated solid-state device (a) Type-I: ITO/polyFe/Gel/ITO, (b) Type-II: ITO/polyFe/Gel/PB/ITO. Corresponding cyclic stability data for (c) Type-I device, and (d) Type-II device stepped between colored state (−1.3 V) and bleached state (+2.7 V) with a 5 s interval.

Table 1
The cyclic performances of Type-I and Type-II devices.

Device[a]	ΔT after 1st cycle (%)	ΔT after 150th cycle (%)	ΔT after 200th cycle (%)
Type-I: ITO/polyFe/Gel/ITO	57.8	56.4 (97.5%)	–
Type-II: ITO/polyFe/Gel/PB/ITO	56.7	54.2 (95.5%)	54.1 (95.4%)

[a] Operation voltage +2.7 V (bleaching), −1.3 V (coloring).

weight loss occurred initially at around 100 °C, which is most probably due to absorbed moisture or acetic acid solvent. After that, it showed quite stable behavior up to 350 °C (22% weight loss).

3.1. Electrochemical and spectroelectrochemical properties of fabricated EC devices

A solid-state electrochromic device was fabricated by using polyFe as an electrochromic layer, $LiClO_4$-based solid PMMA gel as an electrolyte layer, and thin PB as an ion storage counter electrode layer in between two ITO-glass conductive substrates. The details of the device structure are schematically explained in Fig. 2a. The fabricated solid-state electrochromic device showed a vivid bluish-violet color, and upon applying +2.7 V, the color of the device changes from bluish-violet to colorless because of the oxidation of Fe(II) to Fe(III) in polyFe. Similarly, by applying −1.3 V, the device color changes back from colorless to bluish-violet (Fig. 2b), due to the reduction of Fe(III) to Fe (II) in polyFe (Fig. 2b). This reversible color change behavior is stable over several cycles. During the color change of the fabricated solid device, the spectral (T%) change at the oxidized and reduced states was recorded in Fig. 2c. The change in transmittance (ΔT%) between the colored and bleached states was found to be ~57% by monitoring at 580 nm for the singlet MLCT band of polyFe. The dynamic transmittance switching (colored to bleached and vice versa) of the device was monitored over several different intervals (5 s, 2.5 s, 1 s, 0.5 s, and 0.25 s) at a fixed operating voltage of +2.7 V to −1.3 V repeatedly (Fig. 2d). In this study, it was observed that for intervals up to 1 s, the ΔT of the fabricated device remained unchanged. After that, ΔT gradually decreased.

3.2. Effect of counter materials on device performance

Two types of solid-state electrochromic devices were fabricated. One is without any counter material (Type-I), while the other does contain a counter material (Type-II). The Type-I device was fabricated by using polyFe as the electrochromic layer and $LiClO_4$-based semi-solid gel as the electrolyte layer in between two ITO-glass conducting substrates (Type-I: ITO/polyFe/Gel/ITO). The Type-II device was fabricated in the same manner as the Type-I device, but with one extra PB layer on the counter electrode (Type-II: ITO/polyFe/Gel/PB/ITO). The details of the structures of the two types of devices are schematically explained in Fig. 3a (Type-I) and Fig. 3b (Type-II).

The long-term dynamic transmittance behavior of two devices, shown in Fig. 3c (Type-I) and Fig. 3d (Type-II), was recorded by stepping between the colored state (−1.3 V) and bleached state (+2.7 V) with a 5 s interval. The cyclic stability of the fabricated devices was calculated by comparing ΔT at the initial and final stages ($\Delta T_{final}/\Delta T_{initial}$). The ΔT change for the devices initially and after n cycles are summarized in Table 1. As shown, the Type-I device exhibited stable transmittance behavior up to a certain period, after which the stable

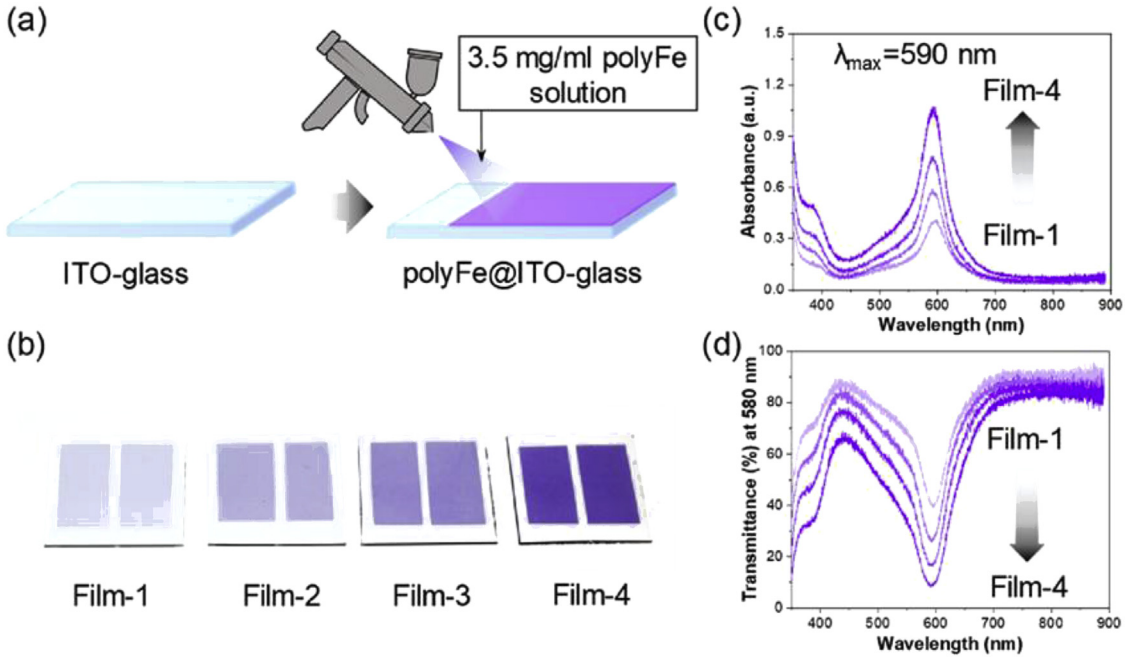

Fig. 4. (a) Schematic presentation of spray coating film preparation, (b) polyFe films of different thicknesses on ITO-glass substrates, (c) absorbance spectra, and (d) corresponding transmittance spectra of the different films.

transmittance behavior suddenly dropped (Fig. 3c). However, the Type-II device exhibited good stable transmittance behavior for a long period of time with only ~4% loss in its properties (Fig. 3d). Due to the presence of an ion storage layer in the **Type-II** device, it showed a steady current flow through the device for a long time, leading to excellent cyclic stability. Therefore, we chose the counter layer-based **Type-II** device for our further studies.

In **Type-I** device, it is supposed that ITO serves as anodic species. The redox mechanism of ITO is not clear, but the reduction of ITO should enable the oxidation of polyFe. However, the reduced state of ITO is not stable so much in the device. We found the ITO in **Type-I** device received damage and changed the color from colorless to brown during the repeated EC changes. It is considered that the damage of ITO decreases the stability of the EC changes.

3.3. Effect of polyFe film thickness on electrochromic properties and EC device

Notably, electrochromic properties greatly depend on the thickness of the electrochromic layer. The spray coating technique was used to make polyFe films of different thicknesses on ITO-glass substrates (Fig. 4a). The film thickness can be nicely controlled by changing the spray speed for a single repetition (Table S1, Supplementary data). Digital photographs of four different films are shown in Fig. 4b (thickness increases left to right). The absorbance and transmittance behavior of the four different thickness films are shown in Fig. 4c and d, respectively. The polyFe films on ITO-glass substrates showed absorbance peak maxima (λ_{max}) at ~590 nm (Fig. 4c), ascribed to the MLCT transition of Fe^{2+} to hexa-coordinated bis-terpyridine ligand of polyFe [19,20]. Film thickness measurements were carried out using a surface profilometer instrument (Fig. S2, Supplementary data). When the thickness was changed from 90 ± 40 nm to 600 ± 100 nm, the film transmittance changed from ~40% to ~9% at the peak maxima at 590 nm (Fig. 4d). With increasing polyFe film thickness, the absorbance of the films gradually increases and naturally the transmittance decreases. Therefore, we optimized film thickness in a certain range where the film shows good electrochromic optical contrast with long-term durability.

To determine the effect of polyFe film thickness on electrochromism, we fabricated four different electrochromic devices with polyFe films of different thickness. The structure of the fabricated devices is already described in Fig. 2a with complete description of each layer. When the film thickness was increased from 90 ± 40 to 600 ± 100 nm, the films became darker in color, as can be seen by the naked eye (Fig. 4b). The change in transmittance (ΔT) and response time (t_b or t_c) increased with increasing polyFe film thickness, however, simultaneously the cyclic performance gradually decreased at room temperature. The continuous dynamic transmittance behavior of four fabricated devices are shown in Fig. 5. All electrochromic performance data for four different solid-state devices are summarized in Table 2. Therefore, considering all electrochromic properties like ΔT, response time, and cyclic stability, we chose the EC device with 240 ± 50 nm film thickness for further study. Coloration efficiency (η) for ECD-4 (the best color contrast device) has been calculated to be 321 cm^2/C from the slope of optical density versus charge density plot (Fig. S3, Supplementary data).

3.4. Temperature stability and performance of fabricated solid electrochromic device

The stability of electrochromic devices at high temperature is an important issue now. To check the thermal stability of our fabricated device, we performed electrochromic operations at room temperature (25 °C), followed by high temperature (50 °C–100 °C), and again at room temperature (25 °C). Therefore, by comparing electrochromic performance before and after high-temperature operation, we could calculate the thermal stability of the EC device. The continuous dynamic transmittance (*T-t*) behavior of the fabricated device before and after different temperature operations are represented in Fig. 6. The *T-t* behavior at 50 °C is clearly demonstrated in Fig. 6a. Initially, the *T-t* performance (100 cycles) was recorded at room temperature (25 °C), followed by another 100 cycles at 50 °C and 40% RH conditions. After that, the same device was subjected to another ~425 cycles at room temperature. Now, comparing the ΔT of the device before and after 50 °C temperature operation, it can be observed that the electrochromic properties were retained at almost ~90% of their original values.

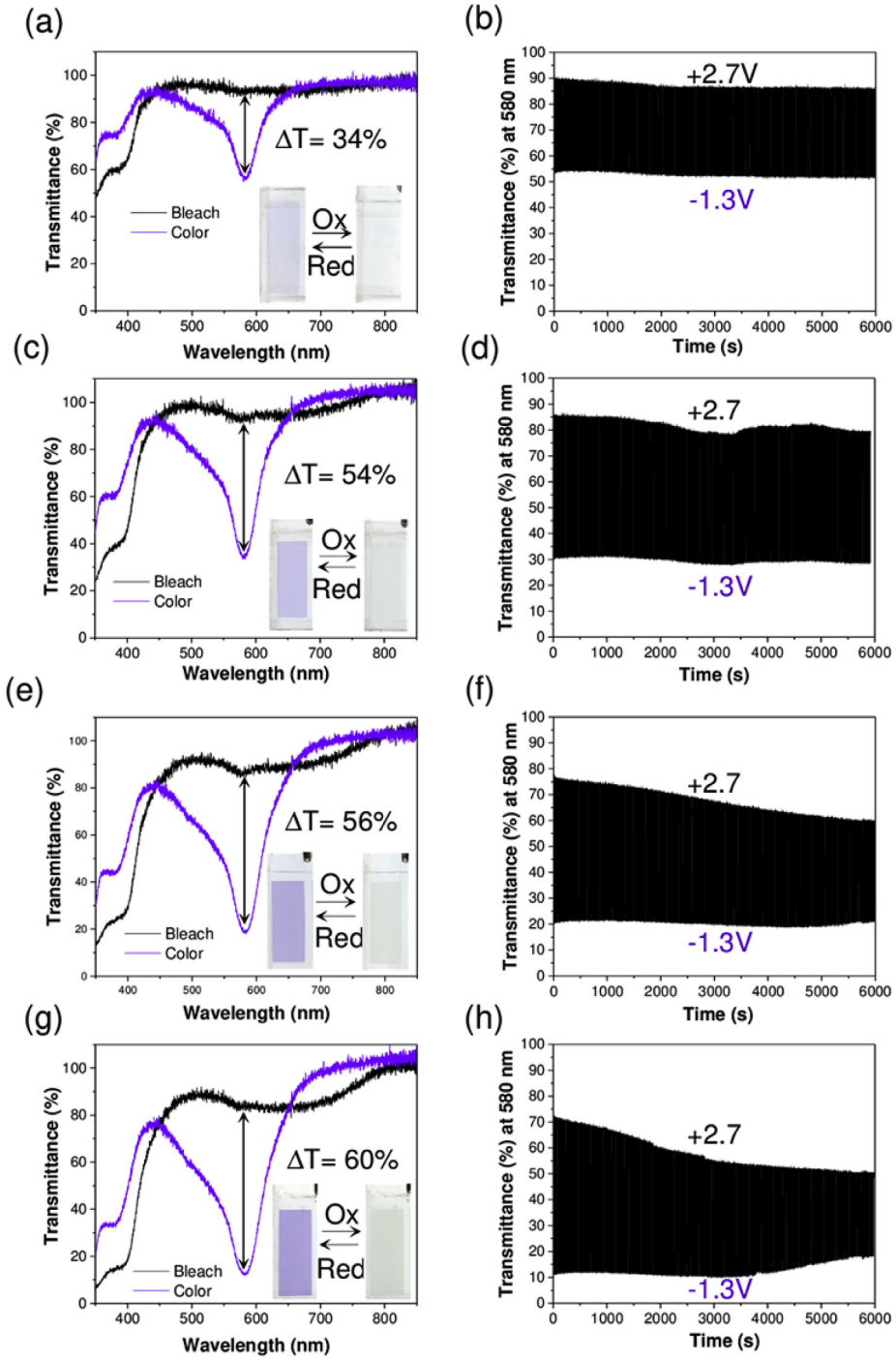

Fig. 5. Spectral transmittance change (left), (inset image represents color change upon applying voltage) and the corresponding long-term cyclic performance (right) of devices based on polyFe films of different thicknesses: (a, b) Device-1, (c, d) Device-2, (e, f) Device-3, (g, h) Device-4. (For interpretation of the references to color in this figure legend, the reader is referred to the Web version of this article.)

Similarly, after electrochromic operation at 60 °C, 70 °C, 80 °C, 90 °C, and 100 °C, we found device stability values of ~78.2%, ~76.3%, ~65.3%, ~55.7%, and 49%, respectively. The electrochromic performance and stability at different temperatures are summarized in Table 3. Therefore, from these results it is shown that as the temperature is increased from 50 °C to 100 °C at a fixed RH (40% RH), the device sustainability gradually decreased. The possible reason for decreasing device performance after high-temperature treatment is gel electrolyte dryness, owing to low ion mobility through the device. The thermal sustainability behavior of the solid electrolyte gel was studied through TGA (Fig. S4, Supplementary data). In the TGA study, the gel electrolyte showed slow weight loss with temperature. At 100 °C, the electrolyte showed ~6% weight loss, probably because of dryness, which affects the ionic conductivity of the gel electrolyte. Before high-temperature treatment, the solid electrolyte showed an ionic conductivity (σ) of $\sim 5.01 \times 10^{-5}\,S\,cm^{-1}$ and during high-temperature operation, the ionic conductivity was enhanced to $\sim 7 \times 10^{-5}\,S\,cm^{-1}$ due to fast ion movement. However, the same gel after cooling down to room temperature showed a decreased ionic conductivity of $\sim 2.9 \times 10^{-5}\,S\,cm^{-1}$ (Fig. S5, Supplementary data). Therefore, due to the low conductivity of the solid gel electrolyte after high-temperature treatment, easy and steady current flow behavior is hampered inside

Table 2
Electrochromic performances of fabricated EC devices with polyFe films of different thicknesses.

Device	PolyFe film thickness (nm)	ΔT%		Response time (t)				Property retained after 1000 cycles[a]
		ΔT% (1st cycle)	ΔT% (1000th cycle)	t_b (s)		t_c (s)		
				1_{st}	1000th	1_{st}	1000th	
1	90 ± 40	34 ± 0.5	34 ± 0.5	0.2	0.3	0.23	0.35	~100%
2	240 ± 50	54 ± 0.5	51 ± 0.5	0.4	0.42	0.51	0.92	~95%
3	360 ± 60	56 ± 0.5	39 ± 0.5	0.6	0.72	0.89	5.0	~70%
4	600 ± 100	60 ± 0.5	33 ± 0.5	0.78	1.05	0.82	> 5	~55%

[a] % of Property retention (ΔT at 1000th cycle/ΔT at 1st cycle) × 100.

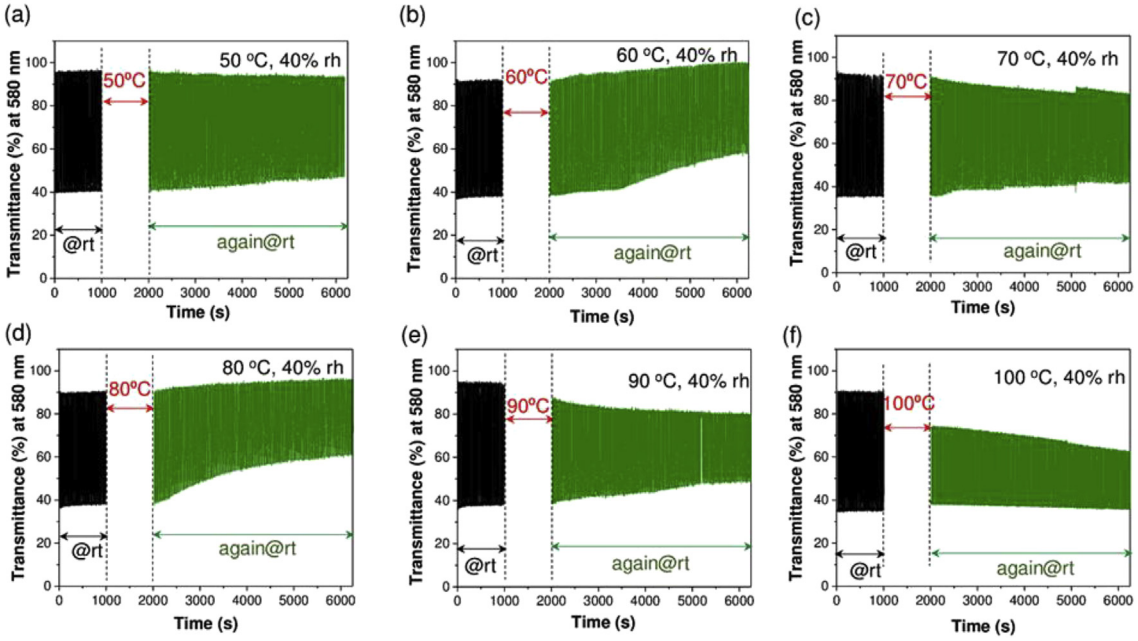

Fig. 6. Transmittance *vs.* time (T-t) behavior of the fabricated electrochromic devices before and after high-temperature operation at (a) 50 °C, (b) 60 °C, (c) 70 °C, (d) 80 °C, (e) 90 °C, and (f) 100 °C at a fixed (~40%) relative humidity.

Table 3
Effect of temperature on electrochromic properties of fabricated solid-state device.

Serial no.	Temp. (°C) and humidity (%RH)	ΔT%		EC property retention[c]
		ΔT%[a]	ΔT%[b]	
1	50 °C, 40% RH	56 ± 0.5	50 ± 0.5	~89.3%
2	60 °C, 40% RH	55 ± 0.5	43 ± 0.5	~78.2%
3	70 °C, 40% RH	55 ± 0.5	42 ± 0.5	~76.3%
4	80 °C, 40% RH	56 ± 0.5	36.5 ± 1	~65.2%
5	90 °C, 40% RH	56.5 ± 0.5	31.5 ± 0.5	~55.7%
6	100 °C, 40% RH	57 ± 0.5	28 ± 0.5	~49%

[a] The change in transmittance before high-temperature EC operation.
[b] The change in transmittance after different high-temperature EC operations.
[c] Property retention (ΔT after high-temperature operation/ΔT before high-temperature operation).

the device, which leads to gradually decreasing performance after high-temperature treatment.

It is considered that for thicker coatings of polyFe the charge capacity of the PB is not sufficient to match the cathodic electrode. In the case, it is supposed that the counter ITO electrode accepts the lacking charge capacity. However, the reduced form of ITO is not so stable in the device, as shown in the Type-I device. It is considered that the cyclic and thermal stability of the Type-II device decreased with increasing the thickness of polyFe more than 230 nm, because the accepted charge capacity of ITO increased.

4. Conclusions

We have successfully fabricated an all-solid-state electrochromic device based on cathodically coloring polyFe as an electrochromic layer on the working electrode, $LiClO_4$-based solid polymeric gel as an electrolyte layer, and anodically coloring PB thin ion storage layer on the counter electrode side in between two ITO-coated glass substrates as a conducting substrate. An automated spray coater machine was used to make polyFe films of different thicknesses on ITO-glass. A facile, low-cost, nontoxic method has been used for device fabrication. The fabricated device showed reversible color change from blueish-violet to colorless and vice versa by applying voltages of +2.7 V and −1.3 V. Counter materials were explored to improve the long-term durability and performance of solid-state devices. We successfully optimized the thickness of polyFe at 240 ± 50 nm with a maximum transmittance change (ΔT) of ~54% (at 580 nm) and 95% property retention after 1000 cycles at room temperature. Importantly, the thermal stability of the fabricated solid device was also studied at different temperatures and we achieved maximum stability at 100 °C with ~50% EC property retention. The idea and concepts described in this study should help to fabricate another kind of electronic device, whose working function and device structure are very similar to electrochromic devices that may operate in hot summer conditions in the future. In addition, we will

investigate the relationship of the applied color and bleach potentials as a function of temperature in the near future, because an over potential may acceralate the degradation of the device at elevated temperatures.

Acknowledgement

This research was financially supported by CREST project (grant number: JPMJCR1533) from Japan Science and Technology Agency.

Appendix A. Supplementary data

Supplementary data to this article can be found online at https://doi.org/10.1016/j.solmat.2019.110000.

References

[1] R.J. Mortimer, D.R. Rosseinsky, P.M.S. Monk, Electrochromic Materials and Devices, Wiley-VCH, Weinheim, 2015, p. 57.
[2] P.M. Beaujuge, J.R. Reynolds, Color control in π-conjugated organic polymers for use in electrochromic devices, Chem. Rev. 110 (2010) 268–320.
[3] G. Cai, J. Wang, P.S. Lee, Next-generation multifunctional electrochromic devices, Acc. Chem. Res. 49 (2016) 1469–1476.
[4] R.J. Mortimer, Electrochromic materials, Chem. Soc. Rev. 26 (1997) 147–156.
[5] W.M. Kline, R.G. Lorenzini, G.A. Sotzing, A review of organic electrochromic fabric devices, Color, Technol. 130 (2014) 73–80.
[6] M. Schott, H. Lorrmann, W. Szczerba, M. Beck, D.G. Kurth, State-of-the-art electrochromic materials based on metallo-supramolecular polymers, Sol. Energy Mater. Sol. Cells 126 (2014) 68–73.
[7] M. Gratzel, Ultrafast colour displays, Nature 409 (2001) 575–576.
[8] C.M. Lampert, Large-area smart glass and integrated photovoltaics, Sol. Energy Mater. Sol. Cells 76 (2003) 489–499.
[9] H. Matsui, T. Hasebe, N. Hasuike, H. Tabata, Plasmonic heat shielding in the infrared range using oxide semiconductor nanoparticles based on Sn-doped In_2O_3: effect of size and interparticle gap, ACS Applied Nano Materials 1 (2018) 1853–1862.
[10] H. Gu, C. Guo, S. Zhang, L. Bi, T. Li, T. Su, S. Liu, Highly efficient, near-infrared and visible light modulated electrochromic devices based on polyoxometalates and $W_{18}O_{49}$ nanowires, ACS Nano 12 (2018) 559–567.
[11] C.G. Granqvist, Electrochromic tungsten oxide films: review of progress 1993–1998, Sol. Energy Mater. Sol. Cells 60 (2000) 201–262.
[12] A. Guerfi, L.H. Dao, Electrochromic molybdenum oxide thin films prepared by electrodeposition, J. Electrochem. Soc. 136 (1989) 2435–2436.
[13] W.H. Nguyen, C.J. Barile, M.D. McGehee, Small molecule anchored to mesoporous ITO for high-contrast black electrochromics, J. Phys. Chem. C 120 (2016) 26336–26341.
[14] Y. Ling, C. Xiang, G. Zhou, Multicolored electrochromism from benzodipyrrolidone-based ambipolar electrochromes at a fixed potential, J. Mater. Chem. C 5 (2017) 290–300.
[15] J. Palenzuela, A. Vinuales, I. Odriozola, G. Cabanero, H.J. Grande, V. Ruiz, Flexible viologen electrochromic devices with low operational voltages using reduced graphene oxide electrodes, ACS Appl. Mater. Interfaces 6 (2014) 14562–14567.
[16] L.-C. Cao, M. Mou, Y. Wang, Hyperbranched and viologen-functionalized polyglycerols: preparation, photo- and electrochromic performance, J. Mater. Chem. 19 (2009) 3412–3418.
[17] A.J.C. Silva, S.M.F. Ferreira, D.D.P. Santos, M. Navarro, J. Tonholo, A.S. Ribeiro, A multielectrochromic copolymer based on pyrrole and thiophene derivatives, Sol. Energy Mater. Sol. Cells 103 (2012) 108–113.
[18] A.A. Argun, P.-H. Aubert, B.C. Thompson, I. Schwendeman, C.L. Gaupp, J. Hwang, N.J. Pinto, D.B. Tanner, A.G. MacDiarmid, J.R. Reynolds, Multicolored electrochromism in polymers: structures and devices, Chem. Mater. 16 (2004) 4401–4412.
[19] F.S. Han, M. Higuchi, D.G. Kurth, Metallo-supramolecular polymers based on functionalized bis-terpyridines as novel electrochromic materials, Adv. Mater. 19 (2007) 3928–3931.
[20] F.S. Han, M. Higuchi, D.G. Kurth, Metallosupramolecular polyelectrolytes self-assembled from various pyridine ring-substituted bisterpyridines and metal ions: photophysical, electrochemical, and electrochromic properties, J. Am. Chem. Soc. 130 (2008) 2073–2081.
[21] C.A. Angell, C. Liu, E. Sanchez, Rubbery solid electrolytes with dominant cationic transport and high ambient conductivity, Nature 362 (1993) 137–139.
[22] V.K. Thakur, G.Q. Ding, J. Ma, P.S. Lee, X.H. Lu, Hybrid materials and polymer electrolytes for electrochromic device applications, Adv. Mater. 24 (2012) 4071–4096.
[23] J. Zhou, J. Wang, H. Li, F. Shen, A novel imide-based hybrid gel polymer electrolyte: synthesis and its application in electrochromic device, Org. Electron. 62 (2018) 516–523.
[24] J. Zhou, J. Wang, H. Li, F. Shen, Hybrid gel polymer electrolyte with good stability and its application in electrochromic device, J. Mater. Sci. Mater. Electron. 29 (2018) 6068–6076.
[25] L.Z. Fan, X.L. Wang, F. Long, All-solid-state polymer electrolyte with plastic crystal materials for rechargeable lithium-ion battery, J. Power Sources 189 (2009) 775–778.
[26] P.T. Jia, W.A. Yee, J.W. Xu, C.L. Toh, J. Ma, X.H. Lu, Thermal stability of ionic liquid-Loaded electrospun poly(vinylidene fluoride) membranes and its influences on performance of electrochromic devices, J. Membr. Sci. 376 (2011) 283–289.
[27] A. Kavanagh, K.J. Fraser, R. Byrne, D. Diamond, An electrochromic ionic liquid: design, characterization, and performance in a solid-state platform, ACS Appl. Mater. Interfaces 5 (2013) 55–62.
[28] D.E. Shen, A.M. Osterholm, J.R. Reynolds, Out of sight but not out of mind: the role of counter electrodes in polymer-based solid-state electrochromic devices, J. Mater. Chem. C 3 (2015) 9715–9725.
[29] K.-M. Lee, H. Tanaka, A. Takahashi, K.H. Kim, M. Kawamura, Y. Abe, T. Kawamoto, Accelerated coloration of electrochromic device with the counter electrode of nanoparticulate Prussian blue-type complexes, Electrochim. Acta 163 (2015) 288–295.
[30] C. Faure, A. Guerfi, M. Dontigny, D. Clément, P. Hovington, U. Posset, K. Zaghib, High cycling stability of electrochromic devices using a metallic counter electrode, Electrochim. Acta 214 (2016) 313–318.
[31] A. Paolella, C. Faure, V. Timoshevskii, S. Marras, G. Bertoni, A. Guerfi, A. Vijh, M. Armand, K. Zaghi, A review on hexacyanoferrate-based materials for energy storage and smart windows: challenges and perspectives, J. Mater. Chem. 5 (2017) 18919–18932.
[32] L.F. Schneemeyer, S.E. Spengler, D.W. Murphy, Ion selectivity in nickel hexacyanoferrate films on electrode surfaces, Inorg. Chem. 24 (1985) 3044–3046.
[33] S.-F. Hong, L.-C. Chen, A red-to-gray poly(3-methylthiophene) electrochromic device using a zinc hexacyanoferrate/PEDOT:PSS composite counter electrode, Electrochim. Acta 55 (2010) 3966–3973.
[34] E. Kholoud, H. Watanabe, A. Takahashi, M.M. Emara, B.A.A.-E. Nabey, M. Kurihara, K. Tajima T. Kawamoto, Cobalt hexacyanoferrate nanoparticles for wet-processed brown–bleached electrochromic devices with hybridization of high-spin/low-spin phases, J. Mater. Chem. C 5 (2017) 8921–8926.
[35] D.M. DeLongchamp, P.T. Hammond, Multiple-color electrochromism from layer-by-layer-assembled polyaniline/Prussian blue nanocomposite thin films, Chem. Mater. 16 (2004) 4799–4805.
[36] E.A.R. Duek, M.-A.D. Paoli, M. Mastragostino, A solid-state electrochromic device based on polyaniline, Prussian blue and an elastomeric electrolyte, Adv. Mater. 5 (1993) 650–652.
[37] T.-H. Lin, K.-C. Ho, A complementary electrochromic device based on polyaniline and poly(3,4-ethylenedioxythiophene), Sol. Energy Mater. Sol. Cells 90 (2006) 506–520.
[38] T.-S. Tung, K.-C. Ho, Cycling and at-rest stabilities of a complementary electrochromic device containing poly(3,4-ethylenedioxythiophene) and Prussian blue, Sol. Energy Mater. Sol. Cells 90 (2006) 521–537.
[39] M. Schott, H. Lorrmann, W. Szczerba, M. Beck, D.G. Kurth, State-of-the-art electrochromic materials based on metallo-supramolecular polymers, Sol. Energy Mater. Sol. Cells 126 (2014) 68–73.
[40] M. Schott, W. Szczerba, U. Posset, A.S. Vuk, M. Beck, H. Riesemeier, A.F. Thünemann, D.G. Kurth, In operando XAFS experiments on flexible electrochromic devices based on Fe(II)-metallo-supramolecular polyelectrolytes and vanadium oxide, Sol. Energy Mater. Sol. Cells 147 (2016) 61–67.